



# Schwann-Cell Autophagy, Functional Recovery, and Scar Reduction After Peripheral Nerve Repair

Po-Yen Ko<sup>1,2</sup> · Cheng-Chang Yang<sup>3</sup> · Yao-Lung Kuo<sup>4</sup> · Fong-Chin Su<sup>1</sup> · Tai-I Hsu<sup>2</sup> · Yuan-Kun Tu<sup>5</sup> · I-Ming Jou<sup>5</sup> 

Received: 12 December 2017 / Accepted: 6 March 2018 / Published online: 11 April 2018  
© Springer Science+Business Media, LLC, part of Springer Nature 2018

## Abstract

The functional outcome after peripheral nerve repair is often unpredictable for many reasons, e.g., the severity of neuronal death and scarring. Axonal degeneration significantly affects outcomes. Post-injury axonal degeneration in peripheral nerves is accompanied by myelin degradation initiated by Schwann cells (SCs), which activate autophagy, a ubiquitous cytoprotective process essential for degrading and recycling cellular constituents. Scar formation occurs concomitantly with nerve insult and axonal degeneration. The association between SC autophagy and the mechanisms of nerve scar formation is still unknown. A rat model of peripheral nerve lesions induced by sciatic nerve transection injuries was used to examine the function of autophagy in fibrosis reduction during the early phase of nerve repair. Rats were treated with rapamycin (autophagy inducer) or 3-methyladenine (autophagy inhibitor). One week after the nerve damage, fibrosis was potently inhibited in rapamycin-treated rats and, based on gait analysis, yielded a better functional outcome. Immunohistochemistry showed that the autophagic activity of SCs and the accumulation of neurofilaments were upregulated in rapamycin-treated rats. A deficiency of SC autophagic activity might be an early event in nerve scar formation, and modulating autophagy might be a powerful pharmacological approach for improving functional outcomes.

**Keywords** Autophagy · Nerve injury · Rapamycin · Neurosurgery · Scarring

## Introduction

Functional recovery and morphological regeneration after peripheral nerve injury are variable: they often leave patients with substantial sensory or motor deficits, and sometimes with chronic pain (Devor and Seltzer 1999). Technological advances in diagnostic imaging, neurosurgical instrumentation, and surgical microscopes

have led to great improvements in diagnosing and repairing transected peripheral nerves; however, the functional outcome after nerve repair is often unpredictable (Robinson et al. 2000). This happens because of the degree of neuronal death (Lundborg and Danielsen 1991) and the formation of scarring and neuromas (aka “neurofibromas”) at the nerve injury site (Lane et al. 1978). Scar formation causes many clinical problems that affect function, growth, and appearance (McCallion and Ferguson 1996). Numerous investigators (Rubinsztein et al. 2005; Larsen and Sulzer 2002; Chu 2006) have studied scar formation after a peripheral nerve injury, and some have tried to modify these events to improve outcomes. However, no therapeutic measures designed to modify scar formation have been introduced into clinical practice.

A growing number of recent reports (Chong et al. 2012; Kim et al. 2013; Ravikumar et al. 2004; Malagelada et al. 2010) highlight the potential importance of autophagy-related processes for aggregating proteins that regulate cell death pathways and regenerate neurons. There are several excellent reviews (McCallion and Ferguson 1996; Rubinsztein et al. 2005; Larsen and Sulzer 2002; Chu 2006) of autophagy in neurons and nerve tissue, and they have inspired us to investigate whether there is any relationship between scar reduction and autophagy.

Yuan-Kun Tu and I-Ming Jou contributed equally to this work.

✉ Yuan-Kun Tu  
edtuyk@gmail.com

✉ I-Ming Jou  
jming@mail.ncku.edu.tw

<sup>1</sup> Department of Biomedical Engineering, National Cheng Kung University, Tainan, Taiwan

<sup>2</sup> Department of Orthopedics, National Cheng Kung University Hospital, Tainan, Taiwan

<sup>3</sup> Institute of Basic Medical Sciences, College of Medicine, National Cheng Kung University, Tainan, Taiwan

<sup>4</sup> Department of Plastic Surgeon, National Cheng Kung University Hospital, Tainan, Taiwan

<sup>5</sup> Department of Orthopedics, E-Da Hospital, Kaohsiung, Taiwan

We chose rapamycin, a lipophilic macrolide antibiotic used in many studies (Chong et al. 2012; Kim et al. 2013; Ravikumar et al. 2004; Malagelada et al. 2010; Caccamo et al. 2010; Rangaraju et al. 2010; Abe et al. 2010; Marinelli et al. 2011), as our autophagy inducer. Rapamycin (aka “sirolimus”) inhibits the mammalian target of rapamycin complex 1 (mTORC1) (Chong et al. 2012), which senses nutrients and negatively regulates autophagy (Kim et al. 2013). Using rapamycin to activate autophagy positively affects Huntington’s (Ravikumar et al. 2004), Parkinson’s (Malagelada et al. 2010), and Alzheimer’s (Caccamo et al. 2010) diseases in animal models, and autophagy dependently improves myelination in neuropathic mouse Schwann cells (SCs) in culture medium (Rangaraju et al. 2010). Relatively few studies have focused on how autophagy is involved in neuronal injury. Gomez-Sanchez et al. (Gomez-Sanchez et al. 2015) reported that autophagy in SCs is crucial for clearing myelin debris during the first 5–7 post-nerve-injury days. Using rapamycin to pharmacologically activate autophagy reduced inflammation, induced analgesia, facilitated nerve regeneration, and prevented chronic pain (Marinelli et al. 2011). Abe et al. (Abe et al. 2010) showed that activating the mTOR pathway regenerated axons in peripheral nerve system neurons.

Although recent studies (McCallion and Ferguson 1996; Rubinsztein et al. 2005; Larsen and Sulzer 2002; Chu 2006; Abe et al. 2010; Marinelli et al. 2011; Gomez-Sanchez et al. 2015) have reported that autophagy benefits peripheral nerve regeneration, few studies (Abe et al. 2010; Marinelli et al. 2011; Gomez-Sanchez et al. 2015) mention whether autophagy is involved in scar reduction or whether the amount of scar tissue created is related to nerve function. Because of the paucity of information on this topic, we investigated in a rat model whether rapamycin is beneficial for myelination and scar modification at nerve repair sites.

## Methods

### Animals and Surgical Procedures

Eight-week-old male Sprague-Dawley rats ( $n = 42$ ) (Biolasco Taiwan, Taipei) were used. They were housed under a 12/12-h light/dark cycle with food and water ad libitum. All procedures followed National Cheng Kung University’s Animal Use Protocol. A sciatic nerve repair model was used with the rats after they had been intramuscularly (i.m.) anesthetized with tiletamine hydrochloride and zolazepam hydrochloride (Zoletil® 50) (80 mg/kg) (Virbac, Carros, France) and premedicated with gentamycin (8 mg/kg [i.m.]) (Yung Shin Pharmaceutical Industrial Co., Taichung, Taiwan). Core temperatures were monitored using rectal probes connected to a multichannel thermometer (Portable Hybrid Recorder, model 3087; Yokogawa Hokushin Electric, Tokyo, Japan) and maintained at 37–38 °C using a heating pad and lamp. Using the

gluteal muscle splitting method, the left sciatic nerve was exposed under a microscope. The rats underwent sciatic nerve transection, and end-to-end epineural nerve repair with 10–0 nylon sutures was performed immediately after transection (Ethilon; Ethicon, Somerville, NJ, USA); the surgical wounds were closed in layers using 3–0 silk sutures.

### Drugs

3-Methyladenine (3-MA; Calbiochem, Hesse, Germany) (500 mg), an autophagy inhibitor, was dissolved in saline (20 ml), and rapamycin (RAPA; Calbiochem) (20 mg) was dissolved in dimethylsulfoxide (DMSO) (20 ml). Immediately after surgery, and daily for 7 days thereafter, the rats were given an ipsilateral hind-paw intraplantar (ipl) injection of the drug (20 ml) assigned to their group. The same solution without RAPA was used as a vehicle control; thus, the control group was injected with DMSO (20 ml) only. As reported elsewhere (Marinelli et al. 2011), the dosage described above did not harm the rats.

### Groups

Twenty-four rats were assigned to the behavioral test and nerve fibrosis assessment group. The remaining 18 rats were assigned to the immunohistochemical analysis group (Fig. 1). In the behavioral test and nerve fibrosis assessment group, the 24 rats were then randomly assigned to 1 of 4 groups ( $n = 6$  in each group): [i] sham neurotomy (control group, given a surgical incision but no sciatic nerve transection, and then injected [ipl] with DMSO); [ii] DMSO (sciatic nerve was transected, repaired, and then injected [ipl] with DMSO); [iii] RAPA (sciatic nerve transected, repaired, and then injected [ipl] with RAPA); and [iv] 3-MA (sciatic nerve transected, repaired, and then injected [ipl] with 3-MA). These 24 rats were killed after they finished the behavioral test to assess nerve fibrosis 56 days after the neurotomy (Fig. 2). To check that the RAPA and 3-MA were really working, the other 18 rats undergoing sciatic nerve repair after transection were randomly assigned to 1 of 3 groups ( $n = 6$  in each group): DMSO, RAPA, and 3-MA as described as above and killed 7 days after neurotomy; their repaired nerves were harvested and then immunohistochemically analyzed.

### Behavioral Test

The 24 rats underwent a walking-track analysis for evidence of neurological compromise 56 days after their neurotomy and drug treatment. The hind-limb footprints of each rat were obtained using a walking track with a video-based system (Fig. 2). (Jen-I et al. 2012; Hsiao-Yu et al. 2012) The walkway is made of a Plexiglas chamber (80 cm long, 6 cm wide, 12 cm high) with a 45° tilting mirror placed under the walkway. The LED light was illuminated from the inferioranterior directions

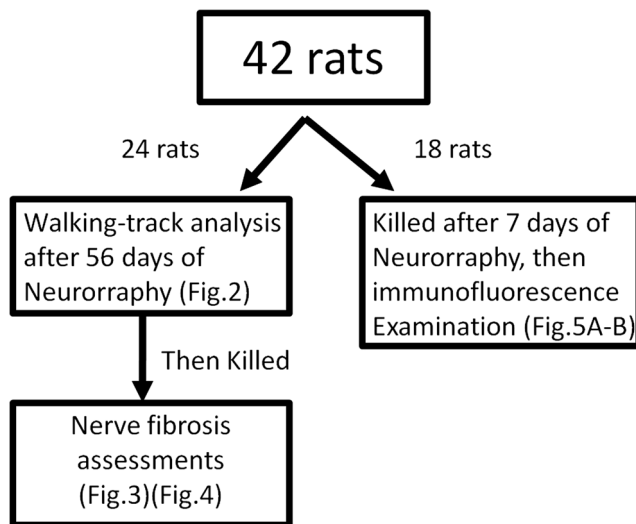


Fig. 1 A flowchart of the study protocol

of the walkway. The tilted mirror reflects the soles on the track. The reflected footprints and lateral limb can be simultaneously recorded by the digital camera (EX-F1; Casio, Japan) positioned 1 m in front of and at the same level as the walkway. The lateral and plantar views of walking track corners were marked with seven red circles (5 mm in diameter) to represent the horizontal and vertical frames, respectively. The data were processed by a MATLAB program designed by our laboratory (MathWorks, Natick, MA). Following an initial pixels/mm calibration, the resolution was 0.18 mm in the 50-cm walking track. For all trials, the system was calibrated to calculate the pixel-to-distance ratio at any plane using red circle markers. The calibration was carried out on

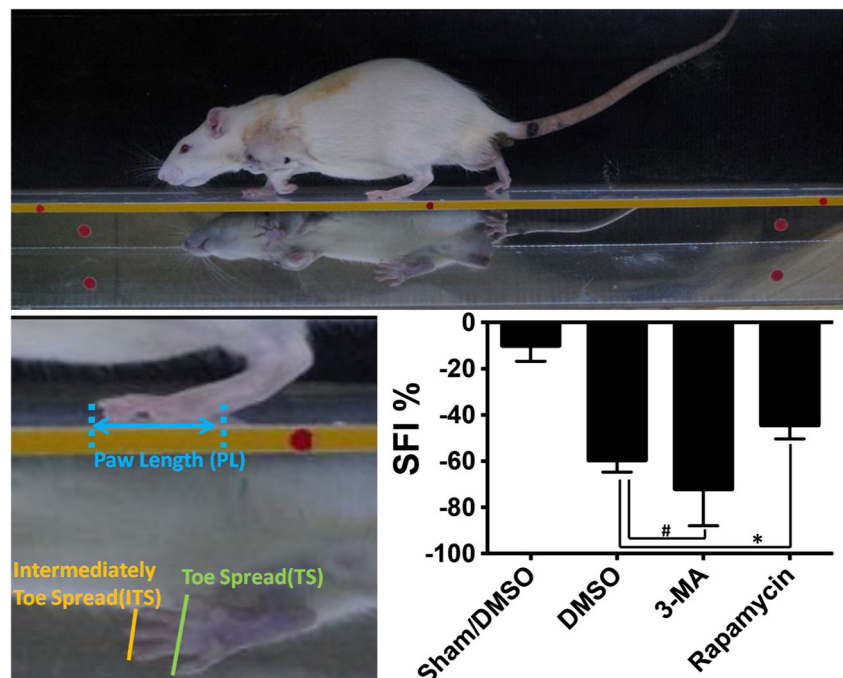
the sagittal and bottom views. The overall pixel to distance ratios were 0.18 and 0.21 mm/pixel for the sagittal and bottom views. The sciatic function index (SFI) (Bain et al. 1989) was calculated using paired measurements of the print length (PL), toe spread (TS) (first to fifth toe), and intermediary toe spread (IT) (second to fourth toe). The measurements of the control left foot (CPL, CTS, CIT) and of the corresponding right experimental foot (EPL, ETS, EIT) were recorded for each rat at each time point. The measurements were then incorporated into the SFI. The formula is as follows:

$$\begin{aligned}
 \text{SFI} = & -38.3[(\text{EPL}-\text{CPL})/\text{CPL}] \\
 & + 109.5[(\text{ETS}-\text{CTS})/\text{CTS}] \\
 & + 13.3[(\text{EIT}-\text{CIT})/\text{CIT}]-8.8
 \end{aligned}$$

### Sciatic Nerve Fibrosis Assessments and Immunohistochemistry

The sciatic nerve fibrosis assessment was done after the walking-track analysis had been completed, and then, the rats were anesthetized with an overdose of sodium pentobarbital (70 mg/kg) (Sigma-Aldrich, St. Louis, MO, USA). After they had been deeply anesthetized, the rats were perfused with 4% paraformaldehyde in phosphate-buffered saline (PBS) for 6 min and then with PBS-only for 6 min. Their sciatic nerves were collected and immersed in 4 °C paraformaldehyde overnight. The next day, after they had been washed with PBS three times for a total of 10 min, the samples were dehydrated with increasing percentages of ethanol (70, 95, and 100%; 1 h at each concentration).

Fig. 2 Sciatic nerve function index (SFI) values in each experimental group. Function recovery was better in RAPA-treated rats than in DMSO- and 3-MA-treated rats. SFI ranged from 10 (normal) to 100 (severe injury). The error bars represent SD. [\*] shows DMSO compared with RAPA, and [#] shows DMSO compared with 3-MA; \**p* < 0.05; \*\**p* < 0.01; \*\*\**p* < 0.005; \*\*\*\**p* < 0.001



The tissue samples were then immersed in xylene, paraffin and an isometric of xylene, and then pure paraffin, in that order. Each nerve was then cut into five 50-mm samples, embedded in paraffin, and then sliced longitudinally into 5-mm-thick sections. Sample sections were deparaffinized using xylene and then rehydrated with decreasing percentages of alcohol (100, 95, and 70%) using a standard protocol (<http://www.abcam.com/protocols/ihc-deparaffinization-protocol>). Nerve sections were stained using a Masson trichrome stain kit (Sigma-Aldrich). Fibrous tissue turned bright blue. For trichrome staining, the hue value used for blue was measured in all slides, and the average hue from 155 to 175 was used to evaluate the slides. The default hue width was used to set an adequate threshold for measuring fibrosis. In this study, the color density was calculated in a 144' 412-pixel photograph and then presented as pixel density/cm<sup>2</sup>. The pixel density was analyzed using Image J 1.46 (<http://imagej.nih.gov/ij/>) as a fibrosis index. For quantitative analysis, type I collagen staining was done in addition to trichrome staining. The slides were prepared using heat-induced antigen retrieval (<http://www.abcam.com/protocols/ihc-antigen-retrieval-protocol>) with 10-mM citric acid (pH 6.0) at 98 °C for 20 min. The slide was incubated with collagen I (EMD; Millipore, Billerica, MA, USA, AB755P; 1:50) antibody overnight at room temperature. After they had been washed, the nerve sections were incubated with goat anti-rabbit IgG antibody (Jackson immunoresearch, 111-035-144; 1:1000) for 1 h. Collagen I was visualized by incubating the sections with diaminobenzidine (DAB). To quantify the percentage of the collagen-I-positive stained area, four photographs of each group around the suture site were acquired and then analyzed using the Image J mark and count tool. Finally, the mean of the collagen-I-positive stained area in each group was calculated.

Seven days after neurotomy, a double-immunofluorescence staining was performed to assess autophagy in specific cell. The sciatic nerve sections were blocked in 2.5% goat serum for 1 h at room temperature following incubation with S-100beta (Abcam, Cambridge, UK, ab212816; 2µg/ml) and neurofilament antibodies (EMD; Millipore, NE1017; 1:1000) overnight at 4 °C, and then washed three times with PBS. The slides were then incubated with light chain 3 (LC3) antiserum which was meant to visualize the ongoing autophagy (PM036; 1:500, MBL Medical & Biological Laboratories, Nagoya, Japan) overnight at 4 °C. After they had been washed, they were double-stained and incubated with Alexa Fluor®594-conjugated goat anti-rabbit IgG (111-585-144, 1:300; Jackson ImmunoResearch, West Grove, PA, USA) and Alexa Fluor®488-conjugated goat anti-mouse IgG (711-545-152, 1:300; Jackson ImmunoResearch, West Grove, PA, USA) for 1 h at room temperature. The slides were mounted (ProLong Gold Antifade Mountant with DAPI; Invitrogen, Waltham, MA, USA) after they had been washed.

All images were captured using fluorescence microscopy (BMI-4000B; Leica Microsystems CMS GmbH, Mannheim, Germany). Image J 1.46 was used to quantify the

immunohistochemical and immunofluorescence assessment results. The number of immunofluorescent pixels was automatically counted (4 nerve sections/rat) using the Image J mark and count tool's RGB (red, green, blue) method, which uses brightness values for the calculation, and then, the mean for each group of rats ( $n = 6/\text{group}$ ) was calculated.

## Statistical Analysis

One-way analysis of variance (ANOVA) was used to compare the SFI, fibrosis index, and immunohistochemical assessment with drug administration after neurotomy. Post hoc comparisons were made using Tukey's test. Significance was set at  $p < 0.05$ . All data are means  $\pm$  standard error of the mean (SEM). Two researchers were not involved in this research and performed all analysis twice.

## Results

### SFI Outcome

The SFI ranges from  $-10$  (normal) to  $-100$  (severe injury) (Bain et al. 1989). The sham group SFI ( $-10.23 \pm 6.54$ ) was unchanged after the rats had been injected (ipl) with DMSO. Rats injected (ipl) with RAPA to induce autophagy had a significantly higher level of hind-limb function ( $-44.56 \pm 5.86$  vs.  $-59.74 \pm 5.11$ ;  $p < 0.05$ ) than did rats injected with DMSO. In contrast, the functional recovery of rats injected (ipl) with 3-MA was significantly inhibited ( $-72.15 \pm 15.84$  vs.  $-59.74 \pm 5.11$ ;  $p < 0.05$ ) (compared with the DMSO group) (Fig. 2).

### Measuring Nerve Fibrosis

To understand the effects of autophagy on sciatic nerve fibrosis, we investigated fibrotic tissue formation after the induction and inhibition of autophagy. Macroscopic observation showed that, 8 weeks after the sciatic nerve repair, the repair site was enlarged (Fig. 3c#) and opaquely dark yellow. The neoplastic (fibrotic) tissue was significantly less abundant in the RAPA group but more abundant in the 3-MA group. Microscopic observation of the fibrosis of the Masson's trichrome-stained sciatic nerve sections showed that the suture site was surrounded by blue-stained fibrotic tissue (\*) (Fig. 3a, b). Sciatic nerves in the DMSO group had significantly more fibrotic tissue around the nerve repair site than did those in the sham group (sham vs. DMSO:  $0.012 \pm 0.004$  vs.  $0.034 \pm 0.005$  pixels per cm<sup>2</sup>;  $p < 0.01$ ) (Fig. 3a, b). Sciatic nerves in the RAPA group had significantly less fibrotic tissue around the nerve-repair site than did those in the DMSO group (RAPA vs. DMSO:  $0.023 \pm 0.003$  vs.  $0.034 \pm 0.005$  pixels per cm<sup>2</sup>;  $p < 0.05$ ), and the sciatic nerves in the 3-MA group



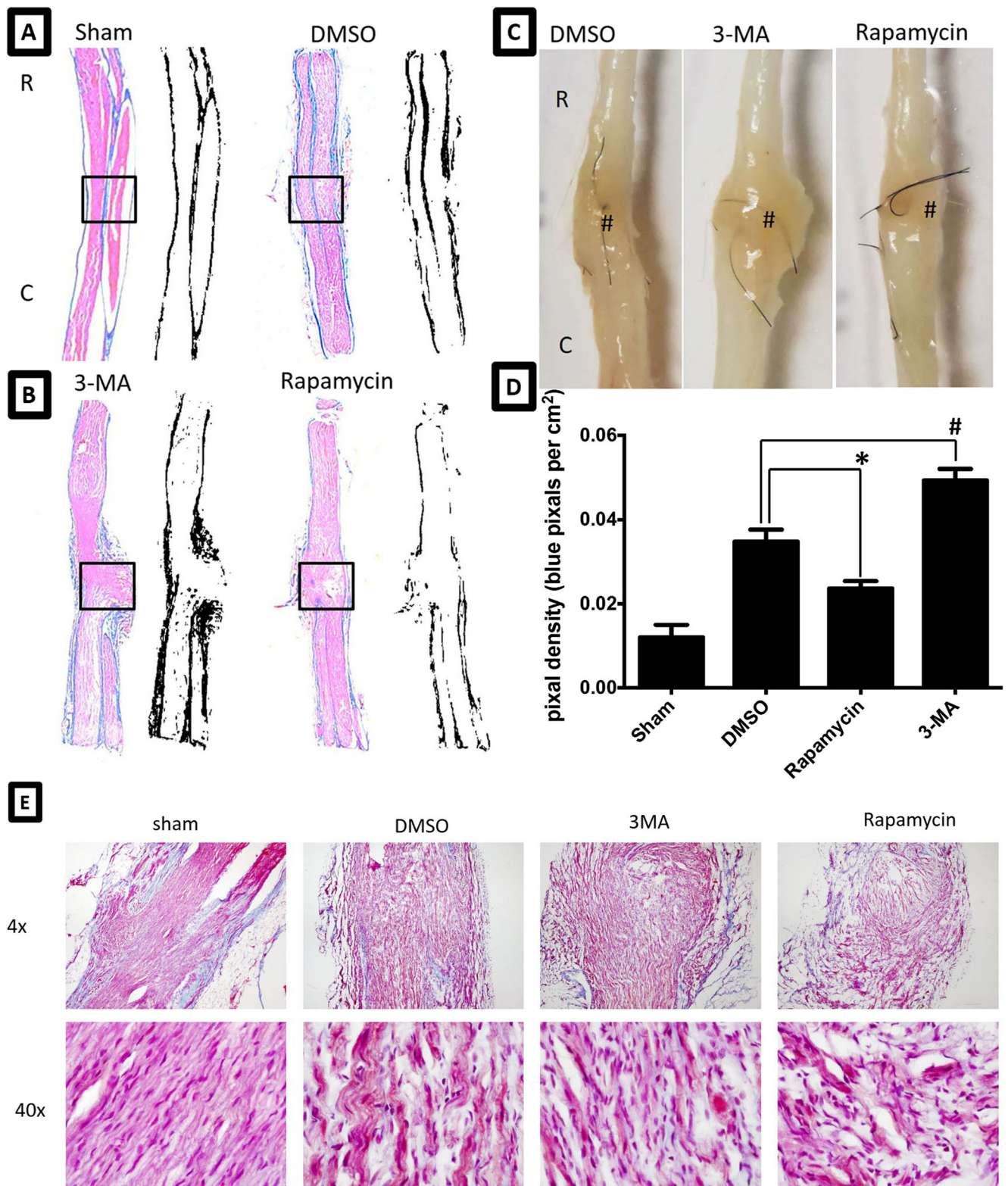


**Fig. 3** The sciatic nerve fibrosis assessment at 2 months after neural repair in **c** gross observation, **a**, **b** Masson's trichrome staining, **d** quantified using the pixel density of fibrotic tissue, and **e** photograph of microscopic magnification 4× and 40× from the suture area (**a**, **b**: □). **f** Enlargement of the magnification 40× from **e**, and arrowheads (△) indicate the Masson's trichrome stained tissue. Autophagy induced by RAPA treatment resulted in greater fibrosis reduction than did DMSO

and 3-MA treatment. The error bars represent SD. #suture site. [\*] DMSO compared with RAPA; [#] DMSO compared with 3-MA; \* $p < 0.05$ ; \*\* $p < 0.01$ ; \*\*\* $p < 0.005$ ; \*\*\*\* $p < 0.001$ . A rat injected with 3-MA shows severe tethering and a very thick scar tissue surrounding the nerve. A rat injected with RAPA shows minimal tethering and only a very thin membrane of scar tissue surrounding the nerve (**e**)

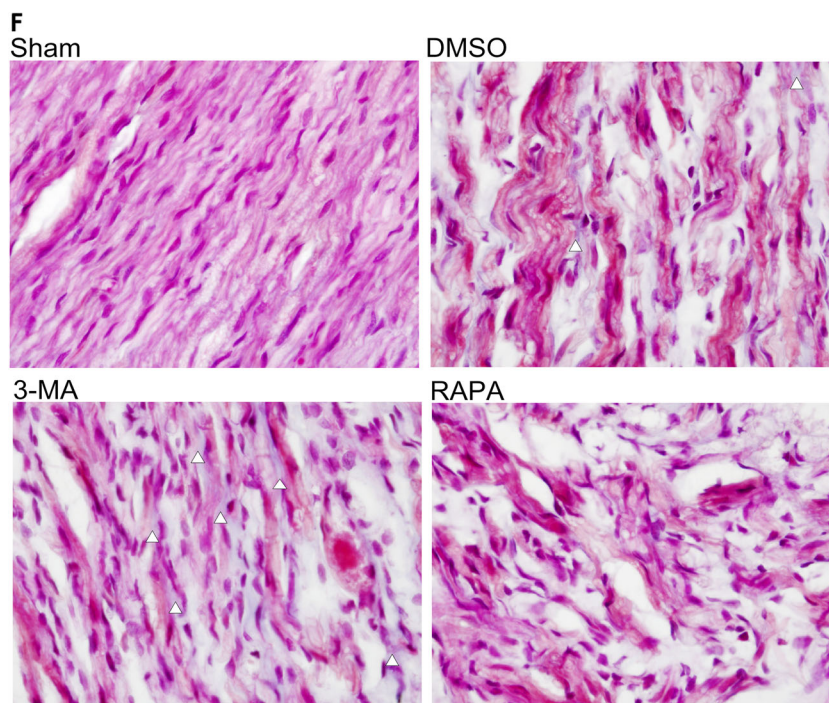


**Fig. 3** (continued)

had significantly more fibrotic tissue than did those in the DMSO group (3-MA vs. DMSO:  $0.049 \pm 0.004$  vs.  $0.034 \pm 0.005$  pixels per  $\text{cm}^2$ ;  $p < 0.05$ ) (Fig. 3d). Collagen I-stained sciatic nerves had a significantly larger distribution area in the 3-MA group and a significantly smaller one in the RAPA group (3-MA vs. DMSO:  $38.49 \pm 3.038$  vs.  $13.91 \pm 2.583\%$ ;  $p < 0.005$ ; RAPA vs. DMSO:  $7.114 \pm 1.909$  vs.  $13.91 \pm 2.583\%$ ;  $p < 0.05$ ) (Fig. 4).

### Sciatic Nerve Immunohistochemistry

Autophagy intensity can be modulated by RAPA or 3-MA (Chong et al. 2012; Kim et al. 2013; Ravikumar et al. 2004; Malagelada et al. 2010; Caccamo et al. 2010; Rangaraju et al. 2010; Abe et al. 2010). Therefore, we investigated whether RAPA increased and whether 3-MA decreased autophagy intensity in neurofilaments and SCs. Seven days after

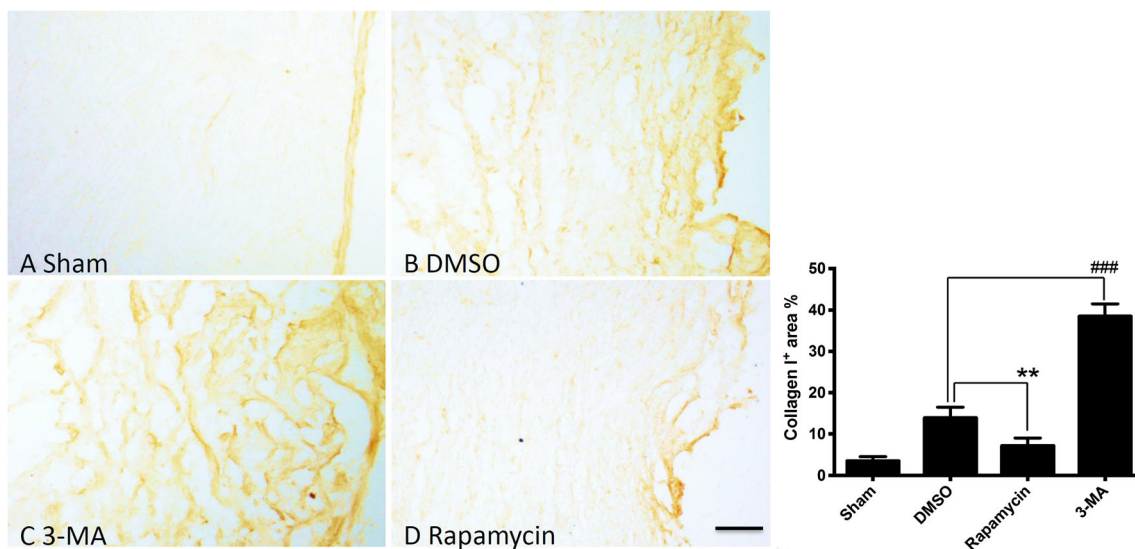


**Fig. 4** Staining with IgG-controlled collagen I. Histograms show the collagen I distribution density. Collagen I expression can indicate fibrosis. Scale bar: 20  $\mu\text{m}$ . [\*] DMSO compared with RAPA; [#]

DMSO compared with 3-MA; \* $p < 0.05$ ; \*\* $p < 0.01$ ; \*\*\* $p < 0.005$ ; \*\*\*\* $p < 0.001$



neurorrhaphy, we immunohistochemically analyzed LC3 expression (autophagy analysis) in the SC (stained with S-100) nerve repair site. SC ongoing autophagy (a merge of S-100 and LC3) in the RAPA group was compared with SC ongoing autophagy in the DMSO and 3-MA groups (Fig. 5a). The RAPA group showed a trend of increasing S-100, LC3, and merge staining. In contrast, the 3-MA group showed a trend of decreasing merge staining (RAPA vs. DMSO:  $115.5 \pm 11.56$  vs.  $28.5 \pm 4.203$  pixels per  $\text{cm}^2$ ,  $p < 0.001$ ; 3-MA vs. DMSO:  $10 \pm 4.546$  vs.  $28.5 \pm 4.203$  pixels per  $\text{cm}^2$ ,  $p < 0.05$ ). There was also a trend of increasing neurofilament, LC3, and merge staining in the RAPA group (Fig. 5b). The 3-MA group showed a decrease of merge staining, however (RAPA vs. DMSO:  $282.6 \pm 14.51$  vs.  $158.8 \pm 30.82$  pixels per  $\text{cm}^2$ ,  $p < 0.001$ ; 3-MA vs. DMSO:  $16.8 \pm 11.12$  vs.  $158.8 \pm 30.82$  pixels per  $\text{cm}^2$ ,  $p < 0.001$ ). In S100 and neurofilament stain samples only, the S100 pixel density (Fig. 5a) was greater in both the 3-MA group and the RAPA group (DMSO [ $57.0 \pm 8.3$ ] vs. 3-MA [ $84.5 \pm 12.0$ ] and RAPA [ $120.6 \pm 10.5$ ] pixels per  $\text{cm}^2$ ). The distribution sites of neurofilament pixel density (Fig. 5b) were not significantly different in the DMSO and the RAPA groups, but they were significantly lower after 3-MA treatment (DMSO vs. 3-MA:  $678.5 \pm 147.4$  vs.  $308.5 \pm 95.0$  pixels per  $\text{cm}^2$ ).

## Discussion

We investigated the effects of autophagy on neuronal scarring in the first 8 weeks after peripheral nerve repair. In rats that had been injected with RAPA, (i) peripheral nerve function recovered more quickly, (ii) fibrosis was inhibited, and (iii) nerve regeneration was facilitated.

As with other conventional wound-healing processes, peripheral nerve regeneration involves an early inflammatory phase, a granulation phase, and, finally, a remodeling phase and scar formation. Thus, it inevitably results in intraneural scarring that impedes axonal regeneration and is a mechanical barrier to sprouting axons (Mathur et al. 1983). Multiple branched axonal terminals were found at the neuromas developed from these barriers (Lane et al. 1978; Sunderland 1978), and the ectopic neural discharge at these sites is important in neuropathic pain (Yates et al. 2000; Devor 2001). An experimental study (Eather et al. 1986) on rat sciatic nerves found that this was most prominent in nerve segments that were 2.5 mm proximal and distal to the injury site. Scar formation also occurred diffusely and distally within the transected nerve, which suggested that this process is not merely a reaction to local inflammation. Moreover, the amount of scar tissue formed depended upon the severity of the nerve trauma (Sunderland 1987). Sunderland's *Nerves and Nerve Injuries* (Sunderland 1987) extensively highlights this scarring problem.

Our rat gait analyses showed that RAPA treatment yielded better functional recovery than did DMSO or 3-MA treatment.

Thus, we hypothesized that functional recovery after sciatic nerve repair is associated with SC autophagy and scar reduction. Autopsies done 2 months after the nerve repair verified our hypothesis. The RAPA group had less scarring and better functional performance. Collagen and scar formation in the distal segment of a severed nerve are associated with the shrinking of endoneurial sheaths, which leads to the reduction of axonal diameter by as much as 80–90% (Sunderland 1987; Sunderland and Bradley 1959). This agreed with Bora's (Bora 1967) report of a negative correlation between the degree of functional return and the amount of scar formation at the repair site.

Immunohistochemistry was used to determine the correlation between SC autophagy and nerve scar reduction. We found that, in the RAPA group, 7 days post-nerve repair, LC3 levels were substantially higher than in the DMSO and 3-MA groups. Co-localization of LC3 (autophagy analysis) protein and S-100 (Schwann cell analysis) was higher in the RAPA group, and these results showed that more SCs were engaged in autophagy in the RAPA group than in the other groups. The co-localization of neurofilaments and LC3 showed that autophagy is beneficial for nerve regeneration. The RAPA group also had more co-localization of neurofilaments and LC3 than did the other groups. Thus, RAPA, which induces autophagy, might facilitate nerve regeneration.

Many studies have investigated the effects of scar-suppressing drugs at a site of peripheral nerve injury. Topically applied triamcinolone acetate, a steroid, improved nerve regeneration in squirrels and monkeys (Graham et al. 1973), and triamcinolone hexacetonide had a similar effect in ferrets (Nachemson et al. 1985). However, the collagen-formation inhibiting agents penicillamine (Bucko et al. 1981) and cis-hydroxyproline (Nachemson et al. 1985) had no apparent effect. Using collagenase (Wehling et al. 1992; Rydevik et al. 2002) and hyaluronic acid (Ozgenel 2003) has produced conflicting results. Other studies report positive results using a polymer gel (Peterson et al. 1996), hyaluronic acid-carboxymethyl cellulose membrane (Adanali et al. 2003), amniotic fluid (Ozgenel and Filiz 2003), low-dose external beam radiation (Gorgulu et al. 2003), tissue plasminogen activator (Zou et al. 2006), and various combinations of these (Ozgenel and Filiz 2004). Here, we tested RAPA, a widely used therapeutic compound that increases autophagy within neuropathic SCs, and that might improve their capacity to myelinate. Many research groups have used RAPA to investigate the effects of SC autophagy on central nervous system diseases like Huntington's (Ravikumar et al. 2004), Parkinson's (Malagelada et al. 2010), and Alzheimer's (Caccamo et al. 2010) and have reported positive effects in animal models. Abe et al. (Abe et al. 2010) reported greater axonal regeneration in peripheral nerve system neurons after they had activated the mTOR pathway with RAPA. Our findings suggest that neural scarring can be reduced and that functional recovery can be increased in an animal model during healing by using RAPA

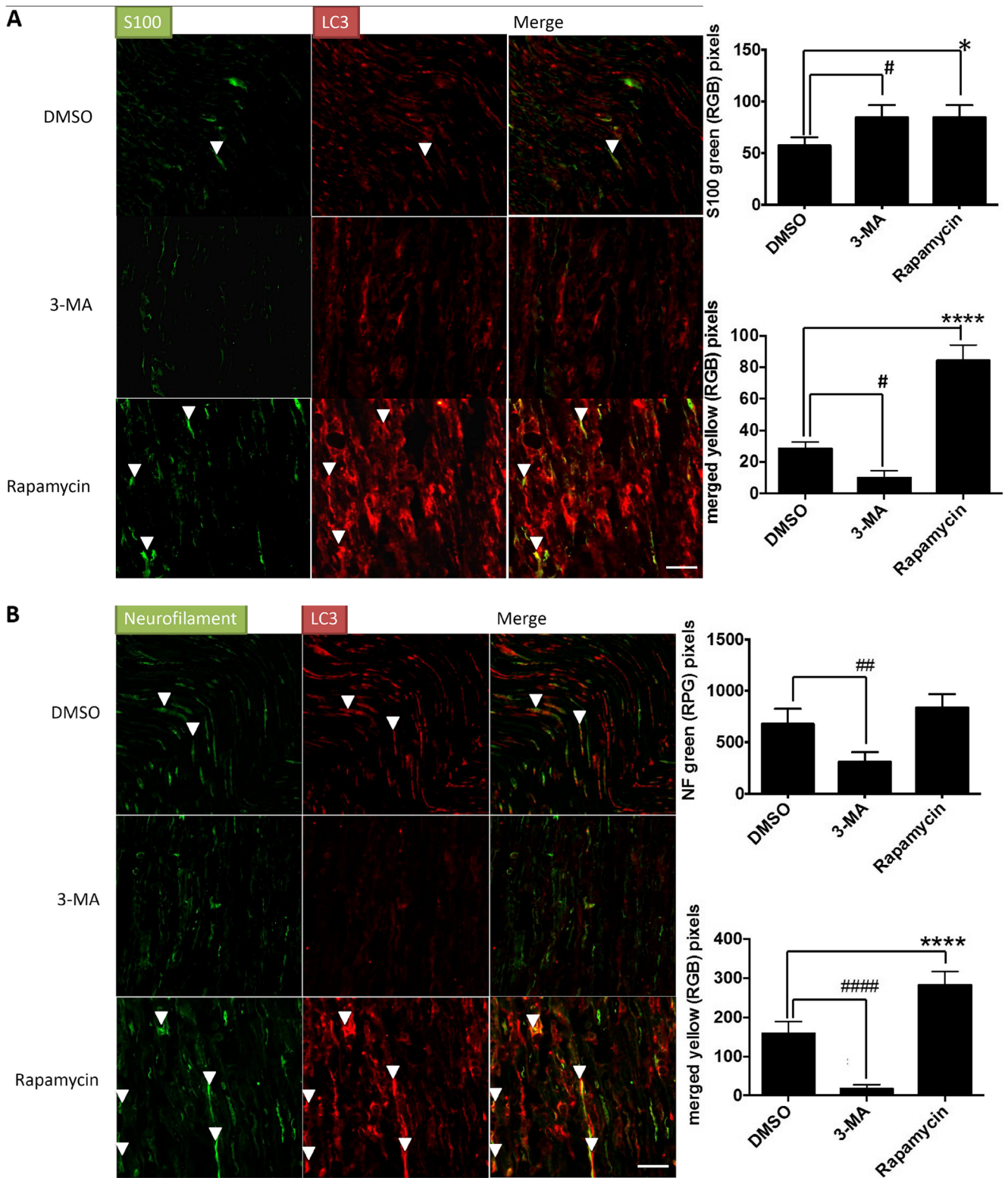


**Fig. 5** A longitudinal section of sciatic nerve immunofluorescence labeled for LC3 (red) with a S-100 (green) and b neurofilament (green) 7 days after sciatic nerve repair. Arrowheads (s) indicate double-positive stained cells. Effects of treatments on LC3 expression are shown in the graph; histograms show red pixels converted to brightness values. The

autophagy intensity was higher in Schwann cells and neurofilaments after RAPA treatment. In contrast, autophagy was inhibited in 3-MA-treated Schwann cells and neurofilaments. Scale bar: 20 mm. [\*] DMSO compared with RAPA; [#] DMSO compared with 3-MA; \* $p < 0.05$ ; \*\* $p < 0.01$ ; \*\*\* $p < 0.005$ ; \*\*\*\* $p < 0.001$



in the first week after nerve repair. Using 3-MA, however, caused neural scarring and worsened functional recovery.

Because SCs respond robustly to RAPA, and because the peripheral nervous system is outside the blood-brain barrier, it is possible that peripheral nerves will respond to this compound more robustly than will nerves in the central nervous system. We showed that RAPA promoted functional recovery and was associated with scar reduction and autophagy. Significantly, RAPA improved the continuity and the neural function of neurofilaments. Our findings support the notion that peripheral nerve regeneration is crucially associated with autophagy and scar reduction.

This study has some limitations. First, we determined pixel density without cell counting. Cell size and staining consistency are the confounding factors for pixel density analysis. Second, although we found that RAPA promoted nerve regeneration and functional recovery, and that nerve regeneration was associated with SC autophagy and scar reduction, we are unable to conclude that autophagy causes nerve regeneration. Additional studies are required to clarify whether autophagy is merely correlated with nerve regeneration, or whether and how it is involved in nerve regeneration.

**Acknowledgements** We are grateful to Kuen-Jer Tsai, PhD, Ms. I-Wen Shene, Ms. Shu Hsien Shih, and Ms. Ying-Chiu Lin for their excellent assistance. None of the authors has a commercial interest relevant to the manuscript.

**Authors' Contributions** Po-Yen Ko and Cheng-Chang Yang contributed equally to this work. Po-Yen Ko and Cheng-Chang Yang carried out the study design, acquiring and analyzing the data, and drafting of the articles; Yao-Lung Kuo, Tai-I Hsu participated in the critical revision of the article for important intellectual content, and technical or logical support; Fong-Chin Su, Yuan-Kun Tu, and I-Ming Jou participated in the final approval of the article provision of the study, obtaining of funding, provision of study materials, and critical revision of the article for important intellectual content. All authors have read and approved the final submitted manuscript.

**Funding** This study was supported by grant NSC106-2314-B-006-004 from the National Science Council, Taiwan, grant EDAHP 106004 from the E-Da Hospital, Taiwan.

## Compliance with Ethical Standards

**Conflicts of Interest** The authors declare that they have no conflict of interest.

## References

- Abe N, Borson SH, Cavalli V et al (2010) Mammalian target of rapamycin (mTOR) activation increases axonal growth capacity of injured peripheral nerves. *J Biol Chem* 285(36):28034–28043
- Adanali G, Verdi M, Tuncel A, Erdogan B, Kargi E (2003) Effects of hyaluronic acid-carboxymethylcellulose membrane on extraneural adhesion formation and peripheral nerve regeneration. *J Reconstr Microsurg* 19:29–36
- Bain JR, Mackinnon SE, Hunter RT (1989) Functional evaluation of complete sciatic peroneal, and posterior tibial nerve lesions in the rat. *Plast Reconstr Surg* 83:129–138
- Bora FJ (1967) Peripheral nerve repair in cats. The fascicular stitch. *J Bone Joint Surg [Am]* 49:659–666
- Bucko CD, Joynr RL, Grabb WC (1981) Peripheral nerve regeneration in primates during D-penicillamine-induced lathyrism. *Plast Reconstr Surg* 67:23–30
- Caccamo A, Majumder S, Richardson A, Strong R, Oddo S (2010) Molecular interplay between mammalian target of rapamycin (mTOR), amyloid-beta, and tau: effects on cognitive impairments. *J Biol Chem* 285:13107–13120
- Chong ZZ, Shang YC, Wang S, Maiese K (2012) Shedding new light on neurodegenerative diseases through the mammalian target of rapamycin. *Prog Neurobiol* 99:128–148
- Chu CT (2006) Autophagic stress in neuronal injury and disease. *J Neuropathol Exp Neurol* 65:423–432
- Devor M (2001) Neuropathic pain: what do we do with all these theories? *Acta Anaesthesiol Scand* 45:1121–1127
- Devor M, Seltzer Z (1999) Pathophysiology of damaged nerves in relation to chronic pain. In: Wall PD, Melzack R (eds) *Textbook of pain*. Churchill Livingstone, London, pp 129–164
- Eather TF, Pollock M, Myers DB (1986) Proximal and distal changes in collagen content of peripheral nerve that follow transection and crush lesions. *Exp Neurol* 92:299–310
- Gomez-Sanchez JA, Carty L, Iruarizaga-Lejarreta M, Palomo-Irigoyen M, Varela-Rey M, Griffith M, Hantke J, Macias-Camara N, Azkargorta M, Aurrekoetxea I, de Juan VG, Jefferies HBJ, Aspichueta P, Elortza F, Aransay AM, Martínez-Chantar ML, Baas F, Mato JM, Mirsky R, Woodhoo A, Jessen KR (2015) Schwann cell autophagy, myelinophagy, initiates myelin clearance from injured nerves. *J Cell Biol* 210(1):153–168
- Gorgulu A, Uzal C, Doganay L, Imer M, Eliuz K, Cobanoglu S (2003) The effect of low-dose external beam radiation on extraneural scarring after peripheral nerve surgery in rats. *Neurosurgery* 53:1389–1395
- Graham W, Patakey P, Calabretta A, Munger B, Buda M (1973) Enhancement of peripheral nerve regeneration with triamcinolone after neurorrhaphy. *Surg Forum* 24:457–461
- Hsiao-Yu L, Tsung-Hsun H, Jia-Jin JC et al (2012) Quantitative video-based gait pattern analysis for hemiparkinsonian rats. *Med Biol Eng Comput* 50:937–946
- Jen-I L, Meng-Yi C, Ming-Long Y et al (2012) Video-based gait analysis for functional evaluation of healing Achilles tendon in rats. *Ann Biomed Eng* 40(12):2532–2540
- Kim SG, Buel GR, Blenis J (2013) Nutrient regulation of the mTOR complex 1 signaling pathway. *Mol Cells* 35:463–473
- Lane JM, Bora FW Jr, Pleasure D (1978) Neuroma scar formation in rats following peripheral nerve transection. *J Bone Joint Surg Am* 60:197–203
- Larsen KE, Sulzer D (2002) Autophagy in neurons: a review. *Histol Histopathol* 17:897–908
- Lundborg G, Danielsen N (1991) Injury, degeneration and regeneration. In: Gelberman RH (ed) *Operative nerve repair and reconstruction*, vol 1. JB Lippincott, Philadelphia, pp 109–131
- Malagelada C, Jin ZH, Jackson-Lewis V, Przedborski S, Greene LA (2010) Rapamycin protects against neuron death in *in vitro* and *in vivo* models of Parkinson's disease. *J Neurosci* 30:1166–1175
- Marinelli S, Pavone F et al (2011) Schwann cell autophagy counteracts the onset and chronification. *Pain* 155:93–107
- Mathur A, Merrell JC, Russell RC, Zook EG (1983) A scanning electron microscopy evaluation of peripheral nerve regeneration. *Scan Electron Microsc* 1983(Pt 2):975–981
- McCallion RL, Ferguson MW (1996) Fetal wound healing and the development of antiscarring therapies for adult wound healing. In:

- Clark RA (ed) The molecular and cell biology of wound repair, 2nd edn. Plenum Press, New York, pp 561–599
- Nachemson AK, Lundborg G, Myrhage R, Rank F (1985) Nerve regeneration after pharmacological suppression of the scar reaction at the suture site. An experimental study on the effect of estrogen-progesterone, methylprednisolone-acetate and cis-hydroxyproline in rat sciatic nerve. *Scand J Plast Reconstr Surg* 19:255–260
- Ozgenel GY (2003) Effects of hyaluronic acid on peripheral nerve scarring and regeneration in rats. *Microsurgery* 23:575–581
- Ozgenel GY, Filiz G (2003) Effects of human amniotic fluid on peripheral nerve scarring and regeneration in rats. *J Neurosurg* 98:371–377
- Ozgenel GY, Filiz G (2004) Combined application of human amniotic membrane wrapping and hyaluronic acid injection in epineurectomized rat sciatic nerve. *J Reconstr Microsurg* 20:153–157
- Peterson J, Russell L, Andrus K, Mackinnon M, Silver J, Kliot M (1996) Reduction of extraneural scarring by ADCON-T/N after surgical intervention. *Neurosurgery* 38:976–983
- Rangaraju S, Verrier JD, Madorsky I, Nicks J, Dunn WA Jr, Notterpek L (2010) Rapamycin activates autophagy and improves myelination in explant cultures from neuropathic mice. *J Neurosci* 30:11388–11397
- Ravikumar B, Vacher C, Berger Z, Davies JE, Luo S, Oroz LG, Scaravilli F, Easton DF, Duden R, O’Kane CJ, Rubinsztein DC (2004) Inhibition of mTOR induces autophagy and reduces toxicity of polyglutamine expansions in fly and mouse models of Huntington disease. *Nat Genet* 36:585–595
- Robinson PP, Loescher AR, Smith KG (2000) A prospective, quantitative study on the clinical outcome of lingual nerve repair. *Br J Oral Maxillofacial Surg* 38:255–263
- Rubinsztein DC, Difiglia M, Heintz N et al (2005) Autophagy and its possible roles in nervous system diseases, damage and repair. *Autophagy* 1:11–22
- Rydevik M, Bergstrom F, Mitts C, Danielson N (2002) Locally applied collagenase and regeneration of transected and repaired rat sciatic nerves. *Scand J Plast Reconstr Surg Hand Surg* 36:193–196
- Sunderland S (1978) Nerves and nerve injuries, 2nd edn. Churchill Livingstone, London, pp 188–200
- Sunderland S (1987) Nerves and nerve injuries. Churchill Livingstone, New York, pp 173–176
- Sunderland S, Bradley KC (1959) Endoneurial tube shrinkage in the distal segment of a severed nerve. *J Comp Neurol* 93:411–420
- Wehling P, Pak M, Cleveland S, Nieper R (1992) The influence of bacterial collagenase on regeneration of severed rat sciatic nerves. *Acta Neurochir* 119:121–127
- Yates JM, Smith KG, Robinson PP (2000) Ectopic neural activity from myelinated afferent fibres in the lingual nerve of the ferret following three types of injury. *Brain Res* 874:37–47
- Yates JM, Smith KG, Robinson PP (2004) The effect of triamcinolone hexacetonide on the spontaneous and mechanically-induced ectopic discharge following lingual nerve injury in the ferret. *Pain* 111:261–269
- Zou T, Ling C, Xiao Y, Tao X, Ma D, Chen ZL, Strickland S, Song H (2006) Exogenous tissue plasminogen activator enhances peripheral nerve regeneration and functional recovery after injury in mice. *J Neuropath Exp Neurol* 65:78–86